EFFECT OF SUBSTRATE TEMPERATURE ON THE TRANSPORT MECHANISMS OF POLYCRYSTALLINE $CdIn_2Te_4$ THIN FILMS GROWN BY THERMAL EVAPORATION

K. YILMAZ[a*], D. GÖLCÜR[a], Y. ÖZCAN[b], D. TAKANOĞLU[a], O. KARABULUT[a]
[a]*Pamukkale University, Arts and Science Faculty, Department of Physics, 20020 Denizli, Turkey.*
[b]*Pamukkale University, Dept. of Electricity and Energy, 20020 Denizli, Turkey.*

In this work, effect of substrate temperature on the conduction mechanisms of thermally evaporated polycrystalline thin films that were grown from sintered $CdIn_2Te_4$ compound were investigated. Temperature dependent conductivity measurements were carried out in the temperature range of 80-400 K to determine dominant current transport mechanisms of the films that were grown at 293 K, 473 K and 573 K substrate temperatures. It was shown that the variation of deposition temperature has considerably altered resistivity and transport properties of the films.

(Received January 17, 2017; Accepted April 3, 2017)

Keywords: Thin films, Thermal evaporation, Conduction mechanism, $CdIn_2Te_4$

1. Introduction

In the last decade, II-VI compounds have been intensively investigated due to their applications in optoelectronics and photovoltaic industry [1-4]. CdTe is one of the most studied compounds of this family since it has a suitable band gap around 1.5 eV for solar energy conversion [5-8]. This compound generally crystallizes in the cubic or hexagonal system and has a defective chalcopyrite structure [4, 9, 10]. It has been reported that as-grown CdTe films are normally rich in Cd vacancies which results in p-type conduction. This is one of the reasons that limit its usage in solar cell applications. When indium atoms are introduced into the lattice of CdTe, they could fill Cd vacancies and/or substitute the Cd atoms in the structure. Thus, this compensation of such vacancies results in n-type conduction. Therefore, ternary $II\text{-}III_2\text{-}VI_4$ compounds such as $CdIn_2Te_4$ have been the subject of many experimental studies for their possible applications in optoelectronic and non-linear optical devices [11-15]. The crystallographic structure, the phase diagram, the electrical properties and the optical properties of $CdIn_2Te_4$ compounds were extensively reported [16-33]. Even though In doped CdTe, CdInTe and $CdIn_2Te_4$ compounds have been widely studied by various researchers, studies on electrical transport properties of polycrystalline $CdIn_2Te_4$ films grown by thermal evaporation method were not reported in literature yet. Thus, the main aim of this work is to investigate transport properties of thermally evaporated polycrystalline $CdIn_2Te_4$ thin films at different substrate temperatures for possible applications of optoelectronic devices.

2. Material and methods

$CdIn_2Te_4$ source compound were sintered by using stoichiometric quantities (1:2:4) of high purity (4Ns) Cd, In and Te elements which have been placed into a chemically cleaned quartz ampoule. The ampoule was sealed after achieving a pressure of about 10^{-4} Torr. Then, the ampoule

*Corresponding author: kyilmaz@pau.edu.tr

was placed in a horizontal, constant temperature zone furnace and heated gently, avoiding over pressures, up to a temperature 1423 K (1150 ^{o}C) higher than the melting points of the elements during 48 hours and then cooled very slowly (10-15 ^{o}C/h). The homogeneity of the compound was achieved by stirring the ampoule occasionally during the heating process. The sintered ingot was crushed into fine grains to obtain evaporation source. Thin films having thicknesses around 1 μm were deposited on chemically and ultrasonically cleaned glass substrates at different substrate temperatures by thermal evaporation technique using a molybdenum boat. The vacuum chamber was evacuated to a pressure of 10^{-6} Torr and the films were deposited around 20-25 A^{o}/s deposition rate which was controlled by Inficon XTM/2 thickness monitor. Several set of samples were produced in order to achieve film reproducibility. For the electrical measurements, ohmic contacts were achieved by thermal evaporation of high purity indium through a mask in Van der Pauw geometry. Then, copper wires attached to the contacts with silver paste. The ohmicity of the contacts was checked during the current-voltage measurements at different temperatures to make sure that the contacts did not add any parasitic impedance to the samples beyond the equilibrium values. The temperature-dependent conductivity measurements for the films deposited at 293 K, 473 K and 573 K were carried out in a Janis closed cycle helium cryostat in the temperature range of 80-400 K by using a Keithley 2400 programmable source-measure unit and a Keithley 2700 electrometer. The temperature was accurately monitored with a Lake-Shore 320 temperature controller during the measurements. Investigated thin films throughout this work were named as B0, B1 and B2 for substrate temperatures 293 K, 473 K and 573 K, respectively.

3. Results and discussion

Temperature dependent conductivity measurements, carried out in the temperature range of 80-400 K, revealed that the conductivity of the films B0, B1 and B2 increased exponentially with increasing temperature which indicates semiconducting behavior of the films, illustrated in Fig. 1. Room temperature resistivity values were found to be 1700 (Ω.cm), 7.8 (Ω.cm) and 0.59 (Ω.cm) for B0, B1 and B2, respectively. Increased substrate temperature of the films resulted in nearly three orders of magnitude decrease in resistivity which confirmed the improved crystallinity in the structure of the film deposited at room temperature. In addition, hot probe technique showed that all the studied thin films exhibited n-type conduction.

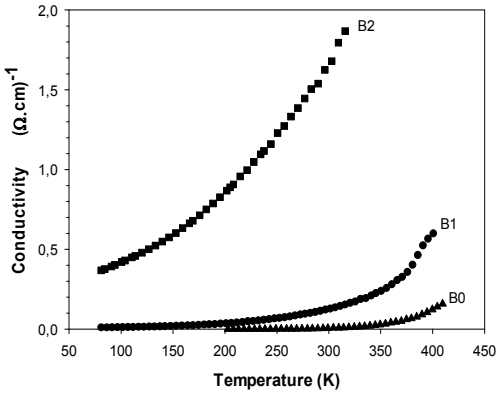

Fig. 1. Conductivity temperature variations of the films B0, B1 and B2 in comparison

In order to determine the dominant conduction mechanisms, the conductivity data was analyzed by the general conductivity expression given below;

$$\sigma = \sigma_0 \exp\left(-\frac{E_a}{k_B T}\right) \quad (1)$$

where E_a is the activation energy, σ_0 is the pre-exponential factor, k_B is the Boltzmann's constant and T is the temperature. The plot of ln(σ) versus inverse temperature for B0 shows a linear variation in the 200-400 K temperature range as shown in Fig.2(a) which indicates that the conductivity obeys the relation given in Eq.(1). The slope of the linear region gives the activation energy E_a = 276 meV. Thus, it can be concluded that in the whole temperature range of 200-400 K the dominant transport mechanism for B0 is thermionic emission of the carriers over the grain boundaries. Due to high resistivity below 200 K, resistivity measurements could not be performed for B0.

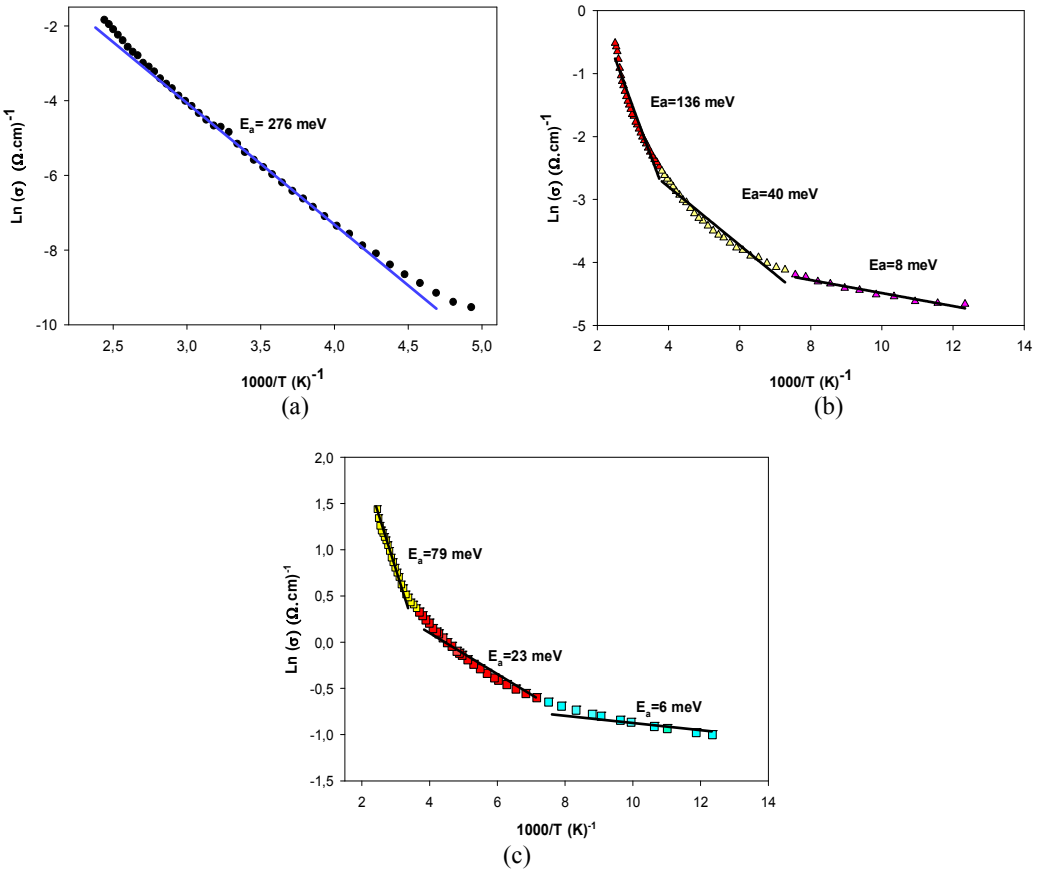

Fig. 2. Ln(σ) versus inverse temperature variations for the films (a) B0 (b) B1 (c) B2

The same analyses were carried out for the films B1 and B2 in 80-400 K temperature range using the advantage of decreased resistivity. Ln(σ) versus inverse temperature variations for both B1 and B2 films indicated three different activation energies at different temperature regions in which different conduction mechanisms were dominant, given in Fig. 2(b) and Fig. 2(c). Activation energies of B1 at low (80-132 K), intermediate (137-267 K) and high (272-400 K) temperature regions were found to be 8 meV, 40 meV and 136 meV, respectively. Whereas for B2, activation energies were found to be 6 meV, 23 meV and 79 meV for low, intermediate and high temperature regions. Since activation energies are greater than the average thermal energy k_BT at 137-400 K temperature region for both B1 and B2, thermionic emission is the dominant conduction mechanism in this temperature region for the films B1 and B2. However, in the low

temperature region calculated activation energies for both B1 and B2 are lower than k_BT which suggests that the conduction mechanism could be Mott's variable range hopping conduction rather than thermionic emission. According to the Mott's theory [34], three-dimensional hopping conduction expression can be given as,

$$\sigma = \sigma_0 \exp\left(-\frac{T_0}{T}\right)^{\frac{1}{4}} \tag{2}$$

where T_0 is a parameter that shows the degree of disorder in the structure and σ_0 is a pre-exponential constant. These two parameters can be expressed as;

$$T_0 = \lambda\alpha^3 \Big/ k_B N(E_F) \text{ and } \quad \sigma_0 = e^2 a^2 \nu_{ph} N(E_F) \tag{3}$$

Where λ is a dimensionless constant at a value of 18.1, α is the decay constant that indicates the rate of fall-off the wave function of an electron at a site, k_B is the Boltzmann's constant, e is the electron charge, a is the variable hopping distance, ν_{ph} is the phonon frequency which was assumed to be 10^{12} s^{-1} and $N(E_F)$ is the density of states around Fermi energy level. T_0 and σ_0 can be found from the plot of Ln(σ) - ($T^{-1/4}$) that is given for B1 and B2, in Fig. 3. The Mott's parameters; R the average hopping distance, and W the average hopping energy can be written as;

$$R = \left[\frac{9}{8\pi\alpha N(E_F) kT}\right]^{\frac{1}{4}} \text{ and } \quad W = \frac{3}{4\pi R^3 N(E_F)} \tag{4}$$

Calculated Mott's parameters for B1 and B2 from Fig. 3, are given in Table 1. The variable range hopping is always to be expected when W >kT and αR>1 with the degree of disorder $T_0 > 10^3$. For the film B1, all conditions for hopping is satisfied for low (80-132 K) temperature region that indicates the dominant conduction mechanism is variable range hopping for which conduction occurs by hopping of the charge carriers to larger distances in order to find energetically closer sites.

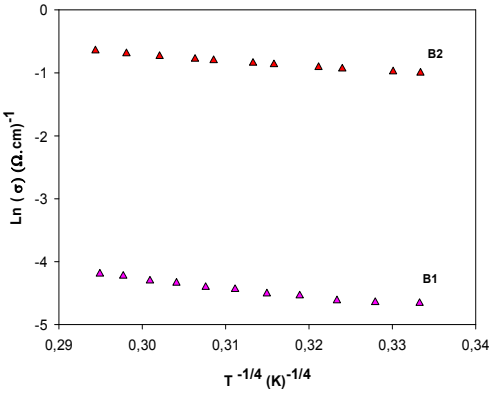

Fig. 3. Ln(σ) - ($T^{1/4}$) variations of the films B1 and B2 in comparison

Table 1. Calculated Mott's parameters for B1 and B2 films

Temperature (80-132 K)	T_0 (K)	α (cm^{-1})	N(E_F) ($cm^{-3}eV^{-1}$)	R (cm)	W (eV)	αR	k_BT (eV)
B1	$2,7x10^4$	$1,7x10^4$	$3,0x10^{13}$	$9,0x10^{-5}$	0,010	1,58	0,009
B2	$6,0x10^3$	$3,8x10^4$	$1,0x10^{15}$	$2,8x10^{-5}$	0,007	1,08	0,009

The disordered atoms create trapping states which are located in the band-gap. In this mechanism, conduction arises from hopping of the charge carriers from the filled trap states to the empty trap states. The empty states can only capture carriers from the filled states below the Fermi level at low temperatures since there are no free carriers to capture from the valence band. However, for the film B2, the Mott's parameters found in Table 1 shows that conditions for hopping were not satisfied for the low temperature region. Thus, we can conclude for B2 that at low temperature region the charge transport may probably be governed by thermally activated tunneling of carriers between localized states, rather than by variable range hopping mechanism.

It can be concluded from the temperature dependent conductivity variations of B0, B1 and B2 thin films that as substrate temperature increases activation energies decreases gradually while conductivity values of the films increase significantly. The source of the extrinsic conductivity is commonly associates with the defect nature of the evaporated thin films. Furthermore, vacuum deposited thin films contain large stresses which result in more trapping centers due to the structural disorder. Increasing conductivity by substrate temperature may be due to improved crystallinity of the film's structure in which some of the defects were removed.

4. Conclusions

Temperature dependent conductivity measurements were carried out in the temperature interval of 80-400 K for the polycrystalline $CdIn_2Te_4$ thin films grown at different substrate temperatures. Conductivity values for all samples increased exponentially with increasing absolute temperature indicating that all films showed semiconducting behavior. Room temperature resistivity values of the films decreased around three orders of magnitude with increasing substrate temperature. At high and intermediate temperatures thermionic emission is the dominant conduction mechanism for all samples with different activation energies.

However, at low temperatures variable range hopping and thermally activated tunneling mechanisms were found to be dominant for the films deposited at 473 K and 573 K, respectively. Temperature dependent conductivity variations of the films showed that as the substrate temperature increases activation energies decreases gradually. This result clearly shows that investigated thermally evaporated films have defective degenerate structures due to structural disorder by which trapping centers are created in the band gap. Increased substrate temperature results in improved crystallinity of the films in which some of the deep trapping centers were cleared out.

Acknowledgements

This work was financially supported by Pamukkale University, Scientific Research Projects Center-BAP (project no:11FBE076).

References

[1] S. Lalitha, S. Zh. Karazhanov, P. Ravindran, S. Senthilarasu, R. Sathyamoorthy, J. Janabergenov, Physica B **387**, 227 (2007).
[2] S. Singh, R. Kumar, K. N. Sood, Thin Solid Films **519**, 1078 (2010).
[3] S. Shanmugan, D. Mutharasu, Mat. Sci. Semicon. Proc. **13**, 298 (2010).
[4] S. Lalitha, R. Sathyamoorthy, S. Senthilarasu, A. Subbarayan, K. Natarajan, Sol. Energ. Mat. Sol. C. **82**, 187 (2004).
[5] J. Fritsche, D. Kraft, A. Thiben, T. Mayer, A. Klein, W. Jaegermann, Thin Solid Films **403-404,** 252 (2002).
[6] H. Bayhan, Ç. Erçelebi, Tr. J. of Physics **22**, 441 (1998).
[7] T. Okamoto, A. Yamada, M. Konagai, Thin Solid Films **387**, 6 (2001).
[8] N. G. Dhere, R. G. Dhere, J. Vac. Sci. Technol. A **23**(4), 1208 (2005).

[9] V. B. Patil, P. D. More, D. S. Sutrave, G. S. Shahane, R. N. Mulik, L. P. Deshmukh, Mater. Chem. Phys. **65**, 282 (2000).
[10] U. P. Khairnar, D. S. Bhavsar, R. U. Vaidya, G. P. Bhavsar, Mater. Chem. Phys. **80,** 421 (2003).
[11] I. Kırbaş, R. Karabacak, Optik, **127**, 7986 (2016).
[12] J. Kiran, R. K. Sharma, S. Kohli, K. N. Sood, A. C. Rastogi, Current Appl. Phys. **3**, 251 (2003).
[13] A.. Shenouda, M.. Rashad, L. Chow, J. of Alloys and Comp. **563**, 39 (2013).
[14] M. Singsa-ngah, A. Tubtimtae, Appl. Phys. A- Mater. Sci. and Proc. **120**, 757 (2015).
[15] M. Singsa-ngah, K. Hongsith, S. Choopun, J. of Colloids and Interface. Sci. **451**, 189 (2015).
[16] S. S. Ou, S.A. Eshraghi, O. M. Stafsudd, A. L. Gentile, J. Appl. Phys. **57**, 355 (1985).
[17] S. Kianian, S.A. Eshraghi, O.M. Stafsudd, A.L. Gentile, J. Appl. Phys. **62**, 1500 (1987).
[18] V. Riede, H. Neumann, V. Kramer, M. Kittel, Solid State Commun. **78**, 211 (1991).
[19] S. A. Lopez-Rivera, L. Martinez, J. M. Briceno-Valero, R. Echeverria, G. Gonzalez de Armengol, Prog. Cryst. Growth Charact. **10**, 297 (1985).
[20] J.C. Woolley, B. Ray, J. Phys. Chem. Solids **15**, 27 (1960).
[21] G. Couturier, B. Jean, J. F. Lambert, P. Joffre, Mater. Sci. Eng. B **21**, 333 (1993).
[22] G. Couturier, A. El Farji, F. Lestournelle, J.C. Launay, J. Appl. Phys. **70**, 4472 (1991).
[23] G. Couturier, B. Jean, J.F. Lambert, P. Joffre, J. Appl. Phys. **73**, 1993 (1813).
[24] S. H. You, K. J. Hong, T. S. Jeong, C. J. Youn, J. S. Park, D. C. Shin, J. D. Moon, J. Cryst. Growth **256**, 116 (2003).
[25] K. J. Hong, S. Y. Lee, S. H. You, J. W. Jeong, J. J. Bang, H. Jian, K. H. Im, AIP Conf. Proc. **700**, 1148 (2004).
[26] S. H. You, K. J. Hong, T. S. Jeong, C. J. Youn, J. S. Park, D. C. Shin, J. D. Moon, J. Appl. Phys. **95**, 4042 (2004).
[27] M. Hong, K. J. Hong, J. Kim, J. Korean Sens. Soc. **15**, 379 (2006).
[28] K. J. Hong, J. Korean Phys. Soc. **45**, 496 (2004).
[29] K. J. Hong, J. Ceram. Process. Res. **6**, 106 (2005).
[30] S. Seto, K. Suzuki, V. N. Abastillas Jr., K. Inabe, J. Cryst. Growth **214/215**, 974 (2000).
[31] W. F. Mohammed, M. A. S. Yousif, Renewable Energy 26 (2002) 285.
[32] M. Zapata-Torres, R. Castro-Rodriguez, A. Martel, Y. P. Mascarenhas, J. Guevara, M. Melendez-Lira, J. L. Pena, J. Vac. Sci. Technol. A **19**(1), 246 (2001).
[33] M. Fuentes-Cabrera, J. Dong, O. F. Sankey, Superficies y Vacio 9 (1999) 310.
[34] N. F. Mott, E. A. Davis, Electronic Process in Non-Crystalline Materials, Clarendon Press, Oxford, 1979.